Comparison of Electron Paramagnetic Resonance Methods to Determine Distances between Spin Labels on Human Carbonic Anhydrase II

Malin Persson,* James R. Harbridge,* Per Hammarström,† Ragheed Mitri,* Lars-Göran Mårtensson,† Uno Carlsson,† Gareth R. Eaton,* and Sandra S. Eaton*

*Department of Chemistry and Biochemistry, University of Denver, Denver, Colorado 80208 USA; and †IFM-Department of Chemistry, Linköping University, Linköping SE-581 83, Sweden

ABSTRACT Four doubly spin-labeled variants of human carbonic anhydrase II and corresponding singly labeled variants were prepared by site-directed spin labeling. The distances between the spin labels were obtained from continuous-wave electron paramagnetic resonance spectra by analysis of the relative intensity of the half-field transition, Fourier deconvolution of line-shape broadening, and computer simulation of line-shape changes. Distances also were determined by four-pulse double electron-electron resonance. For each variant, at least two methods were applicable and reasonable agreement between methods was obtained. Distances ranged from 7 to 24 Å. The doubly spin-labeled samples contained some singly labeled protein due to incomplete labeling. The sensitivity of each of the distance determination methods to the non-interacting component was compared.

INTRODUCTION

Recent advances in site-directed mutagenesis have opened up exciting possibilities for studies of protein structure, folding, and interactions. Cysteines can be introduced at strategic locations in the protein, and attachment of a paramagnetic spin label to the cysteine permits examination via electron paramagnetic resonance (EPR) (Hubbell and Altenbach, 1994; Svensson et al., 1995; Hubbell et al., 1998; Persson et al., 1999). The spin labels are small and have been shown to have minimal effect on protein structure (Mchaourab et al., 1996; Langen et al., 2000). EPR methods have been developed to measure the dipolar interaction between two spin labels and thereby determine the inter-spin distance. Continuous-wave (CW) methods include ratios of peak heights (Kokorin et al., 1972; Sun et al., 1999), the relative intensity of the half-field transition (Eaton et al., 1983a), Fourier deconvolution of dipolar broadening (Rabenstein and Shin, 1995), and computer simulation of line-shapes (Hustedt et al., 1997). Although the dipole-dipole interaction at distances longer than ~20 Å is too small to permit determination of distances from glassy CW spectra with natural isotope-abundance spin labels, these smaller interactions can be measured by pulsed EPR. Pulsed methods include double electron-electron resonance (DEER) (Milov et al., 1981; Larsen and Singel, 1993; Martin et al., 1998; Pannier et al., 2000), the 2 + 1 pulse sequence (Raitsimring et al., 1992), and double-quantum EPR (Saxena and Freed, 1997; Borbat and Freed, 1999).

Each of these methods has been calibrated with different model systems. We seek to compare the distances obtained by these techniques when applied to the well-characterized protein, human carbonic anhydrase II (HCA II), which has a molecular mass of 29.3 kDa (Fig. 1) (Eriksson et al., 1988; Håkansson et al., 1992; Henderson et al., 1976). HCA II catalyzes the conversion of CO_2 to HCO_3^- in erythrocytes (Lindskog, 1997). It consists of a dominating β-sheet made up of 10 β-strands that contains a large hydrophobic cluster and the active site, which is located in a cone-shaped cleft that protrudes 15 Å into the enzyme. Four double-cysteine HCA II variants were constructed by site-directed mutagenesis: N67C/C206 ($HCAII_{67-206}$), V121C/C206 ($HCAII_{121-206}$), N67C/V121C/C206S ($HCAII_{67-121}$), and I59C/A174C/C206S ($HCAII_{59-174}$), and were spin labeled. HCA II has one naturally occurring cysteine in position 206 ($HCAII_{206}$) (Fig. 1). In $HCAII_{67-121}$, and $HCAII_{59-174}$, Cys-206 was replaced by a serine residue. The distance between the β-carbons of the wild-type residues at the mutation sites ranges from 5 to 18 Å (Table 1). Corresponding single-cysteine variants C206 (wild type, $HCAII_{206}$), N67C/C206S ($HCAII_{67}$), and V121C/C206S ($HCAII_{121}$) also were prepared and spin labeled.

MATERIALS AND METHODS

The spin-label 1-oxyl-2,2,5,5-tetramethylpyrroline-3-methyl-methanethiosulfonate (MTSSL) was purchased from Toronto Research Chemicals (North York, Ontario, Canada). Other chemicals were of reagent grade from various commercial sources. Absorbance measurements for protein concentration determinations were performed on a Beckman DU 640 single-beam spectrophotometer. Circular dichroism was measured on a JASCO J-5000 spectropolarimeter.

Site-directed mutagenesis and protein isolation

Substitutions were introduced into the pACA vector (Nair et al., 1991) containing the gene for human carbonic anhydrase II. The mutagenesis was performed either by Kunkel mutagenesis (Kunkel et al., 1987) or with the Quick-Change site-directed mutagenesis kit (Stratagene, La Jolla, CA). To verify the mutations, DNA sequencing was performed by the

Received for publication 17 July 2000 and in final form 28 February 2001.

Address reprint requests to Dr. Sandra Eaton, University of Denver, Department of Chemistry and Biochemistry, 2050 East Iliff Avenue, Denver, CO 80208. Tel.: 303-871-3102; Fax: 303-871-2254; E-mail: seaton@du.edu.

0006-3495/01/06/2886/12 $2.00

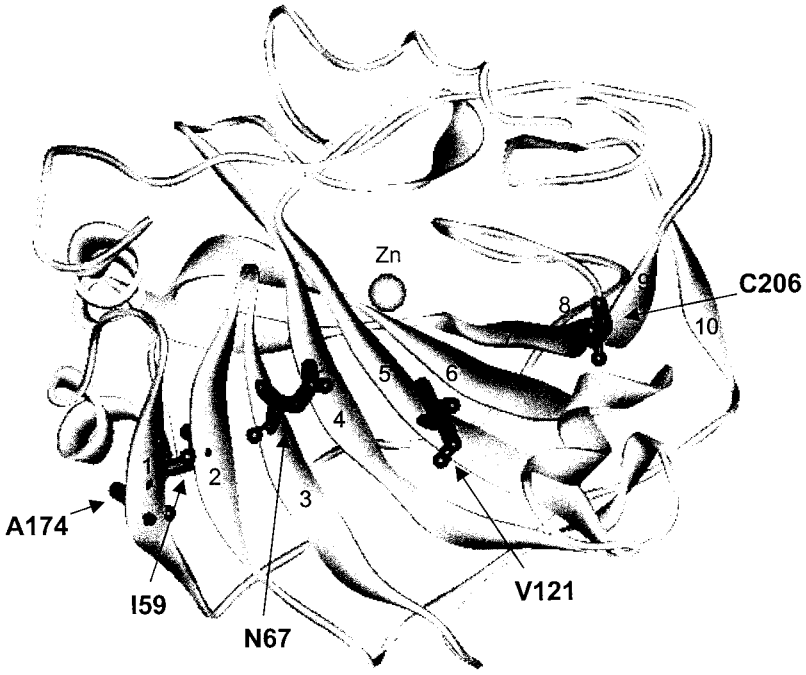

FIGURE 1 Diagram of HCA II x-ray structure (Håkansson et al., 1992). All of the atoms in the naturally occurring amino acids at the positions selected for spin labeling are darkened. For the orientation shown here the side chains on I59 and A174 point into the plane whereas side chains on N67, V121, and C206 point out of the plane.

dideoxynucleotide termination method (Sanger et al., 1977). HCA II and variants thereof were expressed in *Escherichia coli* and were purified by affinity chromatography, as described earlier (Mårtensson et al., 1993).

Spin labeling of HCA II variants

The attachment of spin labels was performed as described earlier (Lindgren et al., 1993) with a few modifications. Briefly, 20 mg of protein was gently stirred overnight at 37°C in a solution (12 ml) containing 0.1 M Tris-H_2SO_4, pH 7.5 (at 37°C), 5 M guanidine hydrochloride (GuHCl), and a 10-fold molar excess of MTSSL over cysteine. The added MTSSL reagent was dissolved in dimethyl sulfoxide (200 μl). The spin-labeled denatured protein was refolded by dilution of the denaturant GuHCl. The protein was added drop-wise to 600 ml of 50 mM sodium phosphate buffer, pH 7.5, at room temperature. The refolding reaction was completed within 2 h at room temperature. The singly spin-labeled variants, $HCAII_{206}$ and $HCAII_{67}$, and doubly spin-labeled $HCAII_{67–206}$ and $HCAII_{59–174}$ were purified by affinity chromatography on a gel matrix with sulfonamide groups that bind efficiently to the active site in HCA II (Khalifah et al., 1977; Mårtensson et al., 1993). In this procedure only the HCA II molecules that possess activity bind to the column, whereas aggregated and misfolded proteins wash through the column. The three HCA II variants that were modified at V121 ($HCAII_{121}$, $HCAII_{121–206}$, and $HCAII_{67–121}$) were not active after spin labeling and refolding and therefore could not be purified on the affinity column. After refolding, these variants were concentrated to 2–3 ml and applied to a Sephadex G-75 superfine (Amersham Pharmacia, Piscataway, NJ) size exclusion column (60 ml) previously equilibrated with 50 mM sodium phosphate buffer, pH 7.5. The spin-labeled HCA II variants eluted in three baseline-separated peaks that correspond to aggregated, misfolded, and native protein, respectively. For proteins prepared by either purification method, the native conformation was confirmed by the characteristic near-UV circular dichroism spectrum (Freskgård et al., 1994). To check the effect of purification technique on sample integrity, portions of a sample of $HCAII_{67–206}$ were purified by both size exclusion and affinity chromatography. The EPR and CD spectra of the two preparations were indistinguishable. Typical yields were 2–3 mg

TABLE 1 Distances determined from EPR spectra

Doubly spin-labeled variant	Distance between β-carbons (Å)*	Half-field transition Å	Fourier deconvolution Å	Line shape simulation Å	DEER Å
$HCAII_{67-121}$	8.8	7		7–8	
$HCAII_{59–174}$	5.4	8	8.5–9	9–10	
$HCAII_{121-206}$	10.9		16–18	14–15†	18 (70%)
				17–19‡	24 (30%)
$HCAII_{67–206}$	17.9		17–20		20 ± 1.8

*Distance between β-carbons of native amino acids at the sites where substitution with cysteine was performed, calculated from the X-ray crystal structure (Håkansson et al. (1992).

†Including unconstrainted contribution from singly labeled protein.

‡Assuming 100% doubly labeled protein.

of purified spin-labeled protein. For EPR spectroscopy, solutions were concentrated to 0.2–0.73 mM protein (based on A_{280}, ϵ_{280} = 54,800 M^{-1} cm^{-1} (Nyman and Lindskog, 1964)). Purification and concentration were performed at 4°C. For low-temperature EPR studies, 100 μl of protein solution was mixed with an equal volume of glycerol placed in a 4-mm-outer-diameter quartz tube and rapidly frozen in liquid N_2. For the doubly labeled variants the final spin concentration, after addition of glycerol, typically was ~0.2–0.4 mM and the protein concentration was 0.1 to 0.2 mM. Samples of each variant were prepared twice and stored in liquid nitrogen.

Assays of activity and cysteine concentration

Carbonic anhydrase activity was measured with a CO_2 hydration assay (Rickli et al., 1964; Freskgård et al., 1991). Free cysteine concentrations in samples denatured with 5 M GuHCl were assayed with 4,4′-dithiodipyridine (Grassetti and Murray, 1967). Before spin labeling the assay detected 80–110% of expected cysteine concentrations. After spin labeling, up to 20% unreacted cysteine was detected.

CW-EPR measurements

EPR spectra were recorded on a Varian E9 X-band (9.1–9.2 GHz) spectrometer with a TE_{102} resonator and quartz variable temperature dewar insert. Samples for room temperature (19–22°C) spectroscopy were contained in 1-mm-internal-diameter capillaries. Four scans (200 G wide) at a microwave power of 2 mW and a 1-G modulation amplitude were signal averaged. At 108 K, a GaAsFET preamplifier was used to improve the signal-to-noise ratio, and spectra were recorded at 200- or 400-G scan widths with 0.005-mW microwave power and 0.5- or 1.0-G modulation amplitude at 100 kHz, averaging four or eight scans. Half-field transitions were recorded by averaging 32 scans of 200 G, centered at 1642 G, at a microwave power of 200 mW and a modulation amplitude of 6.3 G. In the region of the half-field transition, a background spectrum (buffer mixed with an equal volume of glycerol and frozen) was recorded under the same conditions as the sample and subtracted digitally.

Double electron-electron resonance (DEER)

The four-pulse DEER experiments were performed at 77 K on a locally constructed spectrometer (Quine et al., 1987; Rinard et al., 1999) using the procedure of Pannier et al. (2000). The resonator is a TE_{102} resonator with an enlarged iris coupling hole to permit extensive over-coupling. The second microwave frequency was generated with a Wavetek Microsweep model 965 source. The frequency difference between the two sources was set to 60 MHz, and the two frequencies were adjusted to be symmetrically positioned with respect to the resonant frequency of the over-coupled rectangular resonator (ν = 9.145 GHz, Q ≈ 100). The lengths of the pulses at ν_1 were 15 and 30 ns. The π pulse at ν_2 was 30 ns long, which corresponds to a B_1 of ~6 gauss. The magnetic field was adjusted such that the observed signal (ν_1) was on the low-field edge of the nitroxyl signal and the perturbing pulse at ν_2 was in the center of the nitroxyl signal, thereby maximizing the impact of the perturbing pulse. The constant timing, τ, of the pulses that generated the observed echo was selected to minimize proton modulation. In principle, the optimum τ would be an integer multiple of the reciprocal of the proton Larmor frequency. It was found that small adjustments in τ values were required to minimize proton modulation, presumably due to the use of finite pulse lengths and inherent system timing delays. The value of τ was 643 ns for doubly labeled $HCAII_{67–206}$ and 947 ns for doubly labeled $HCAII_{121–206}$. The timing, T, of the perturbing pulse was varied from $-\tau$ to $+\tau$ ns in steps of 6 ns. A total of 250 scans were recorded with a pulse repetition time of 200 μs. A background signal recorded with no power in the perturbing pulse was subtracted.

Data analysis

Spin labeling efficiency

Spin-labeling efficiency (SLE) is defined as the ratio of the nitroxyl spin concentration to the concentration of cysteines. Doubly integrated EPR signal intensities were calculated and compared with double integrals of spectra of a nitroxyl standard (tempone, Aldrich, Milwaukee, WI) at both room temperature and at 108 K to determine spin concentrations. The cysteine concentration was calculated from A_{280} and the number of cysteines per mole of each variant. If it is assumed that the labeling efficiency is the same for both sites in a doubly labeled protein; then the probability that both sites are labeled is $(SLE)^2$ and the probability that either site is labeled is $2(SLE)(1 - SLE)$. Because there are two labels per mole of protein in a doubly labeled protein and because there is no EPR signal from unlabeled protein, the fraction of the EPR signal for a double-cysteine variant that is due to doubly spin-labeled protein is $2(SLE)^2/[2(SLE)^2 + 2(SLE)(1 - SLE)] = SLE$, and the fraction of intensity due to singly labeled protein is $1 - SLE$. Thus, in the spectrum of a double-cysteine variant, if the fraction of the total intensity due to sharp components of the spectrum equals $1 - SLE$, then this signal can be assigned to singly labeled protein. A larger contribution from the sharp component indicates the presence of a conformation with an inter-spin distance that is so long that it is indistinguishable from non-interacting label by CW spectroscopy.

The peak height ratio

The peak height ratio, d_1/d, was determined from the low temperature (108 K) spectra as shown in Fig. 2 (Kokorin et al., 1972; Sun et al., 1999).

Intensity of half-field transition

The relative intensity of the half-field transition (Fig. 2 *A*) compared with that of the allowed transitions was calculated by taking the ratio of the double-integrated signal intensities, corrected for differences in number of scans, modulation amplitude, and microwave power. The distance was calculated as previously reported (Eaton et al., 1983a).

Fourier deconvolution of line-shape broadening

This technique, described by Rabenstein and Shin (1995), compares spectra of a doubly labeled variant and corresponding singly labeled variants. Spectra of the three singly labeled HCA II variants were similar to each other, but not identical. For analysis of each of the doubly labeled variants, spectra of two singly labeled variants were combined, with correction for differences in spin concentration and observing frequency, and then baseline corrected. The Fourier transform of the spectrum of the doubly labeled sample was divided by the Fourier transform of the combined spectrum of the singly labeled variants to produce the Fourier transform of the broadening function (Figs. 3, *C* and *D*; 4 *D*; and 5 *B*). Only the real component of the Fourier transform is displayed because the early portion of the imaginary component was approximately zero, provided the input spectra were properly corrected for differences in frequencies at which spectra were recorded. A Gaussian curve was fit to the broadening function, and that fit function was reverse-Fourier transformed to provide the function from which the inter-spin distance was calculated (Rabenstein and Shin, 1995). A Gaussian is a convenient approximation for the Fourier transform of the dipolar coupling pattern (Ottemann et al., 1998). For each sample, deconvolutions were done for data obtained with 0.5- and 1.0-G modulation amplitudes and for combinations of singly and doubly labeled samples from different preparations. As noted by Rabenstein and Shin (1995), the information concerning the broadening is at the beginning of the Fourier-transformed array, and noise dominates the

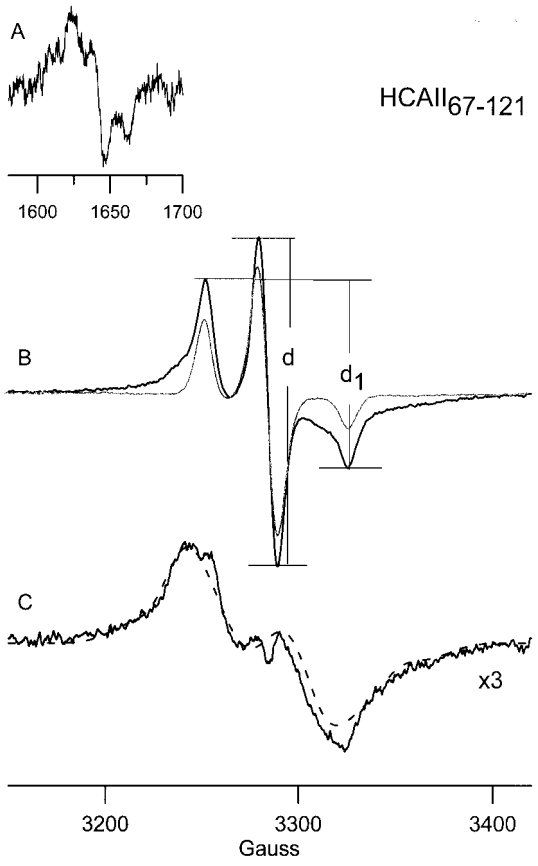

FIGURE 2 X-band (9.21 GHz) EPR spectra at 108 K in glassy 1:1 buffer:glycerol. (*A*) The half-field transition for $HCAII_{67-121}$ with a spin concentration of 0.29 mM; (*B*) Allowed, g~2 transitions (——) for doubly spin-labeled $HCAII_{67-121}$ with a spin concentration of 0.29 mM shown at ×5 the *y*-axis amplification used for the sum of the spectra for the corresponding singly labeled $HCAII_{67}$ and $HCAII_{121}$ (*light line*); (*C*) Spectrum of $HCAII_{67-121}$ (——) after subtraction of contribution from singly labeled protein and simulation obtained for $r = 8$ Å (— — —). The *y*-axis amplification in *C* is ×3 that for the doubly labeled sample in *B*.

remainder of the array. Singly spin-labeled analogs of $HCAII_{59-174}$ were not prepared. Deconvolutions of the spectra of doubly labeled $HCAII_{59-174}$ were performed with combinations of spectra for the three singly labeled variants that were prepared. The dipolar-broadened component of the spectrum of doubly labeled $HCAII_{59-174}$ is so broad that the deconvoluted broadening functions were essentially independent of the choice of singly labeled analog.

The cutoff frequency for determination of the Gaussian fit function was varied, and the distances reported in Table 1 are the ranges observed for several cutoff frequencies applied to several experimental data sets. For initial data sets of 2048 points, typical cutoff frequencies were at points 20–50 in Fourier space (Figs. 3, *C* and *D*; 4 *D*; and 5 *B*). A given cutoff frequency was deemed to be acceptable if two criteria were met: 1) the resulting Gaussian fit was in good agreement with the initial portion of the data, often including a good fit extending beyond one or more noise spikes that occurred at higher frequency than the cutoff, and 2) the ratio of the limiting (baseline) value to the initial value (data point 0) was greater than or equal to (1 − SLE), within experimental uncertainty.

Simulation of the line-shapes

Simulations were performed with programs developed by Hustedt and co-workers (Hustedt et al., 1993, 1997) that employ automated search routines to determine best-fit parameters. The *g* and *A* values obtained for the singly labeled samples with the program Rigid were $g_{xx} = 2.0086–2.0084$, $g_{yy} = 2.0052–2.0057$, $g_{zz} = 2.0020–2.0022$, $A_{xx} = 4.84–6.47$, $A_{yy} = 4.45–5.40$, and $A_{zz} = 37.32–38.16$ G, which are in good agreement with literature values (Hustedt et al., 1997). The algorithm in Rigid simulates line-widths as a combination of Gaussian and Lorentizan contributions. To obtain a measure of line-widths that could be more directly compared for different samples, spectra also were simulated with the locally written program, Monmer, which is based on the algorithms described in Toy et al. (1971). The resulting peak-to-peak widths for a Gaussian first-derivative line-shape were 7.0 G for $HCAII_{206}$, 7.5 G for $HCAII_{67}$, and 10.1 G for $HCAII_{121}$.

In simulations of the spectra of immobilized dipolar-coupled nitroxides using the Hustedt et al. (1997) programs, the average of the parameters for the two singly labeled variants were used as fixed inputs. Input parameters that could be varied in the simulations include line-widths, inter-spin distance, and angles that define the relative orientation of the *g*- and *A*-matrices for the two nitroxides and the orientation of the inter-spin vector (Hustedt et al., 1997). Calculations with the simulated annealing program Safit were performed four to six times for each spectrum of a doubly labeled sample. From the sets of parameters generated by the simulated annealing, ones with lower values of χ^2 (sums of deviations) were input into a Marquardt-Levenberg routine (Dipolar) that calculates a spectrum for comparison with the experimental spectrum (Hustedt et al., 1997). The program option diprig was selected for most of the simulations, because it includes a variable contribution from singly labeled sample, in addition to the dipolar-coupled signal. The changes in parameters during the Marquardt-Levenberg optimization were much smaller than changes produced by the simulated annealing. For both steps of the simulations, calculations were performed in which the Gaussian broadening and line-width of the spin-coupled signal were either fixed at the values observed for singly labeled variants or allowed to vary. Simulations in which the best-fit Gaussian broadening or line-width was smaller than for the corresponding singly labeled variants were rejected. Increases in broadening or line-width compared with the singly labeled variants may be due to distributions of orientations. These programs were applied to original data, rather than to files from which the contribution of singly labeled contribution had been subtracted, to avoid potential bias introduced by imperfect subtractions.

Simulations also were performed with the locally written program Meno (Eaton et al., 1983b), which does not include automated search routines but permits input of different *g*, *A*, and line-width parameters for the two spin-labeled sites. To test the parameters for the spin-spin interaction that were obtained by the automated search routines, spectra were calculated using Meno and compared with experimental spectra from which the contributions from singly labeled protein had been subtracted (Figs. 2 *C*, 3 *B*, and 4 *B*).

Analysis of DEER data

The four-pulse DEER data (Fig. 6) were simulated (Milov et al., 1998) assuming that all possible orientations of the inter-spin vector relative to the external magnetic field were randomly sampled. A Gaussian distribution of inter-spin distances (Pannier et al., 2000) was assumed, and the width of the distribution was adjusted to match the damping of the modulation. The fraction of spins perturbed by the pulse at the second frequency was adjusted to match the initial depth of the modulation. To check the performance of our hardware and data analysis, four-pulse DEER experiments were performed for the anthraquinone diradical studied previously by Larsen and Singel (1993) and for the biradical denoted as 3 by Pannier et al. (2000). For both of these samples the distances and distribution widths obtained from our data are in good agreement with results reported by Pannier et al. (2000).

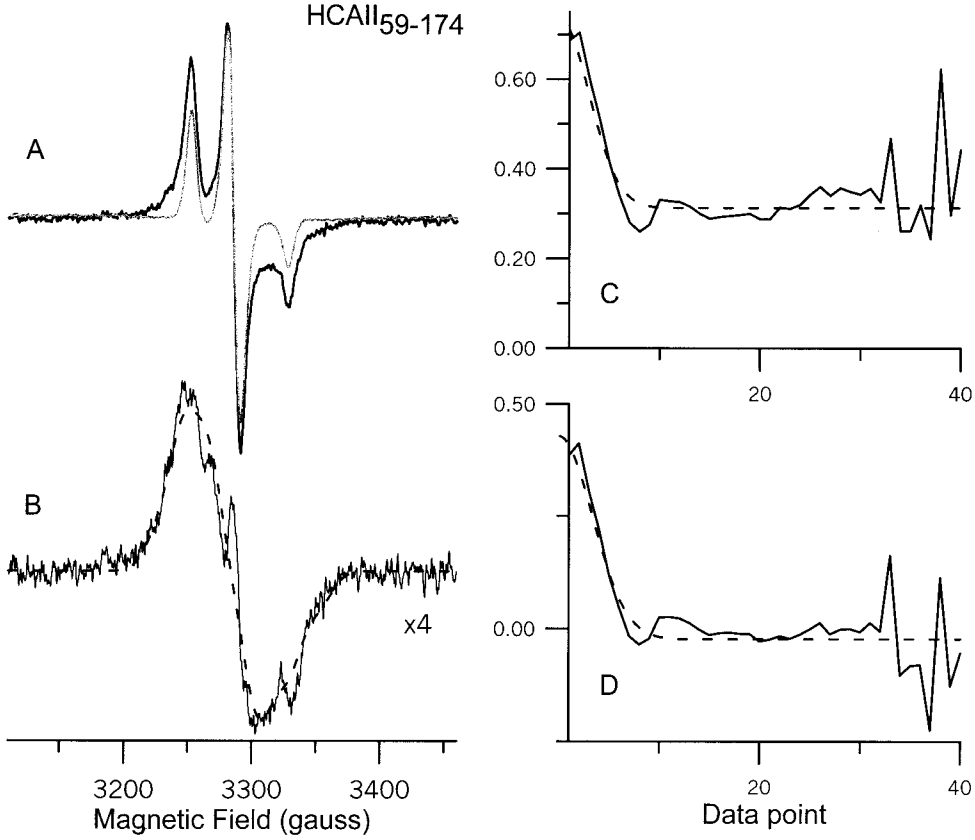

FIGURE 3 X-band (9.21 GHz) EPR spectra at 108 K in glassy 1:1 buffer:glycerol. (*A*) Doubly spin-labeled $HCAII_{59-174}$ with a spin concentration of 0.31 mM (——) shown at ×4 the *y*-axis amplification as used for the sum of the spectra for singly labeled $HCAII_{121}$ and $HCAII_{206}$ (*light line*); (*B*) Spectrum of $HCAII_{59-174}$ (——) after subtraction of contribution from singly labeled protein and simulation obtained for $r = 9$ Å (— — —). The *y*-axis amplification in *B* is ×4 that for the doubly labeled sample in *A*. (*C* and *D*) Real part of the Fourier transform of the broadening functions for doubly spin-labeled $HCAII_{59-174}$ (*C*) and for doubly spin-labeled $HCAII_{59-174}$ (*D*) after subtraction of the contribution from singly spin-labeled protein. The values of *r* calculated from the broadening functions were 8.6 and 8.8 Å for the curves in *C* and *D*, respectively. The cutoff point for calculating the Gaussian fit was data point 50 for both curves, which is well into the noisy portion that is not displayed in this figure.

RESULTS AND DISCUSSION

Spin labeling of HCA II variants

The positions selected for spin labeling are buried in the hydrophobic cluster of HCA II (Fig. 1); therefore, variants were spin labeled in the denatured state and then allowed to refold. For both the singly and doubly labeled variants, circular dichroism spectra exhibited features characteristic of native HCA II. Because the near-UV circular dichroism spectrum of HCA II is very complex, this spectrum is a sensitive fingerprint of the native conformation (Freskgård et al., 1994). The CD spectra strongly suggest that all of the variants had a native-like structure, even though variants spin-labeled at V121C were not catalytically active. Although changing Val-121 to Cys-121 did not interfere with activity, attachment of the MTSSL to Cys at this location made these variants inactive. Val-121 in the native protein is part of the hydrophobic cluster facing the active site cleft (Nair et al., 1991). This hydrophobic cluster has been shown to be important for the activity of the enzyme (Fierke et al., 1991; Alexander et al., 1991). The MTSSL attached at position 121 may protrude into the active site cleft and hinder access of the CO_2 molecule, or it may disturb the coordination to the Zn^{2+} ion in the active site (Hunt et al., 1999). The broader EPR line-shape for spin-label in $HCAII_{121}$ than in $HCAII_{67}$ or $HCAII_{206}$ indicates that the label at this location samples a wider range of solvent polarity than at the other two sites, which suggests a wider range of conformations at this site.

Assays for free cysteine and measurement of spin label concentrations by EPR, combined with protein assays based on A_{280}, indicated that spin labeling efficiencies were 60–90%, with some variation between individual preparations. If the labeling were randomly distributed between the two cysteines, these labeling efficiencies would result in mixtures in which 60–90% of the EPR signal intensity is due to doubly labeled protein. These samples therefore provide a test of the ability of various methods to determine inter-spin distances in the doubly labeled protein in the presence of the sharper lines due to singly labeled protein.

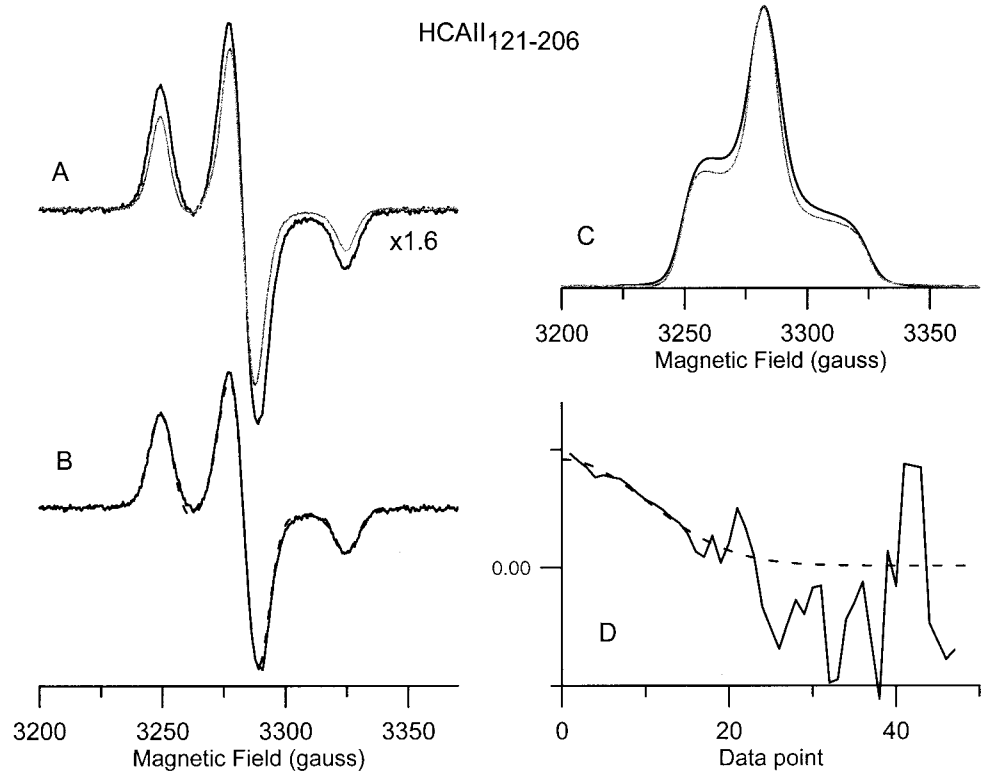

FIGURE 4 X-band (9.21 GHz) EPR data at 108 K in glassy 1:1 buffer:glycerol. (*A*) Doubly labeled $HCAII_{121–206}$ with a spin concentration of 0.26 mM (——) shown at ×1.6 the *y*-axis amplification used for the sum of spectra of singly labeled $HCAII_{121}$ and $HCAII_{206}$ (*light line*); (*B*) Spectrum of $HCAII_{121–206}$ after subtraction of contribution from singly labeled-protein (——) plus simulation (— — —) obtained with $r = 16.5$ Å and the same *g* values and line-widths as observed for the corresponding singly labeled variants; (*C*) First integrals of spectra shown in part *A*, with *y*-axis scale adjusted to match peak heights; (*D*) Real part of the Fourier transform of the broadening function for $HCAII_{121–206}$ (——) calculated after subtraction of the contribution from singly labeled protein. The Gaussian fit function in *D* (— — —) was calculated with a cutoff at point 20 and corresponds to $r = 16.1$ Å.

EPR Spectra

Room-temperature EPR spectra of the four doubly spin-labeled carbonic anhydrase variants in buffer solution (Fig. 7) demonstrate that the spin labels are substantially immobilized. Differences in extents of label immobilization at different positions on the protein make it difficult to compare the impact of electron spin-spin interaction on the fluid-solution spectra. However, the broadening in the wings of the spectra decreases from top to bottom of Fig. 7, which is the order of increasing inter-spin distance obtained from measurements in immobilized samples (Table 1). EPR spectra of the doubly labeled variants in glassy 1:1 buffer: glycerol solutions at 108 K (Figs. 2–5) exhibited differences that were more readily interpreted than the fluid-solution spectra. The broader signals for $HCAII_{67–121}$ (Fig. 2) and $HCAII_{59–174}$ (Fig. 3) than for $HCAII_{121–206}$ (Fig. 4) and $HCAII_{67–206}$ (Fig. 5) indicate shorter inter-spin distances for the former variants than for the latter. The distances that were obtained for the four doubly spin-labeled variants are summarized in Table 1 and are discussed in the following paragraphs.

From the peak height ratio, d_1/d (Fig. 2), the extent of broadening of the spectrum can be estimated (Kokorin et al., 1972; Sun et al., 1999). For singly labeled protein or doubly labeled protein with an inter-spin distance greater than ~20 Å, a value of <0.4 is expected (Korkorin et al., 1972). For the singly labeled variants of HCA II the values of d_1/d were as follows: $HCAII_{206}$, 0.36; $HCAII_{67}$, 0.37; and $HCAII_{121}$, 0.45. The large value of d_1/d for $HCAII_{121}$ is due to the large line-widths, mentioned above. For the doubly spin-labeled variants the values of d_1/d were as follows: $HCAII_{59–174}$, 0.59; $HCAII_{67–121}$, 0.55; $HCAII_{121–206}$, 0.46; and $HCAII_{67–206}$, 0.39. Comparison of the trend in these ratios with the trends in the distances obtained by other methods (Table 1) indicates only qualitative agreement. The d_1/d method is particularly sensitive to interference from contributions due to singly labeled proteins because the sharper lines from non-interacting label tend to dominate the peak height ratios. For example, for $HCAII_{67–121}$ (Fig. 2 *B*), subtraction of the contribution from singly labeled proteins reveals a severely broadened spectrum (Fig. 2 *C*) for which it would be difficult to calculate a value of d_1/d.

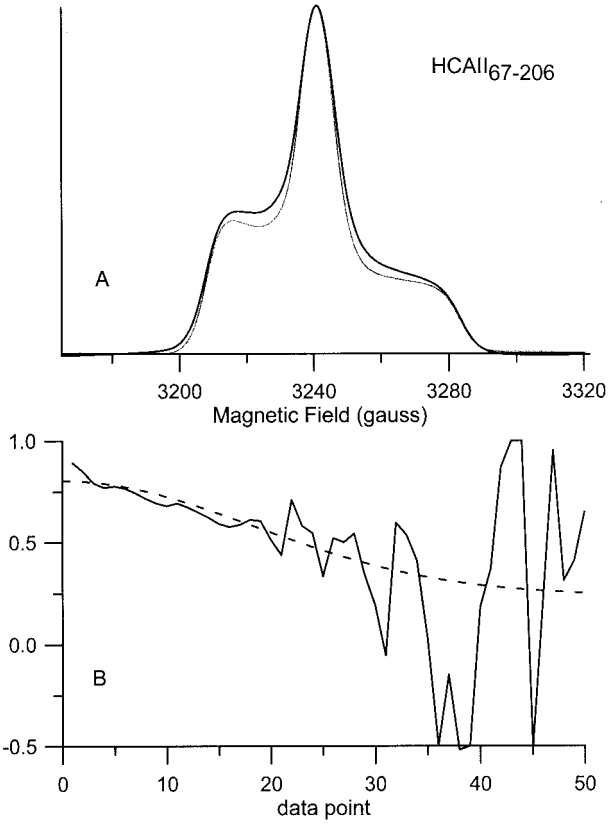

FIGURE 5 X-band (9.10 GHz) EPR data at 108 K in glassy 1:1 buffer: glycerol. (*A*) First integral of spectra for doubly labeled $HCAII_{67–206}$ with a spin concentration of 0.26 mM (——) superimposed on the sum of spectra of singly labeled $HCAII_{67}$ and $HCAII_{206}$ (*light line*), with *y*-axis amplification adjusted to match peak heights; (*B*) Real part of the Fourier transform of the broadening function for $HCAII_{67–206}$ (——). The Gaussian fit in *B* (— — —) was calculated with a cutoff at point 30 and corresponds to a distance of 19.6 Å.

Thus, the value of d_1/d determined from the spectrum in Fig. 2 *B* is not a reliable indicator of the inter-spin distance for $HCAII_{67–121}$.

Distance between labels at positions 67 and 121

The substantially higher amplification required to obtain a spectrum of $HCAII_{67–121}$ with amplitude comparable to that for the sum of the singly labeled variants (Fig. 2 *B*) indicates a relatively short inter-spin distance. The two spin labels attached to $HCAII_{67–121}$ are close enough to allow determination of the distance (7 Å) from the ratio of the intensities of the forbidden half-field transition and the allowed $g \approx 2$ transitions (Fig. 2) (Eaton et al., 1983a). When the Fourier deconvolution method (Rabenstein and Shin, 1995) was applied to the data for $HCAII_{67–121}$, the broadening function in Fourier space decayed rapidly, as expected for a short inter-spin distance. However, the calculated distance was strongly dependent on the cutoff frequency. The distance for this sample may be too short for the deconvolution method to work well.

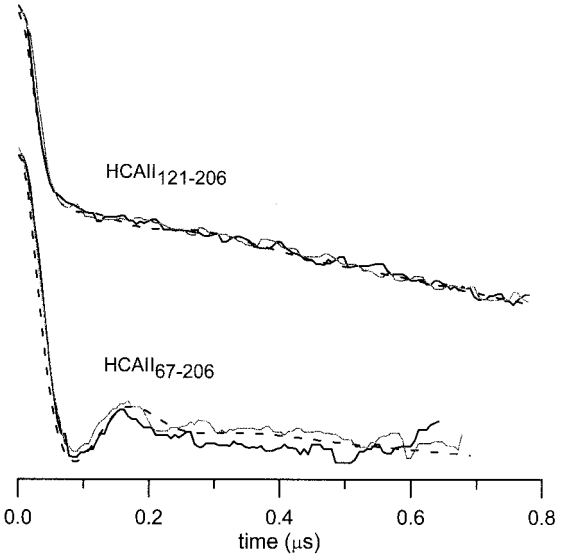

FIGURE 6 X-band (9.15 GHz) four-pulse DEER data obtained at 77 K for doubly spin-labeled $HCAII_{121–206}$ with a spin concentration of 0.88 mM and doubly spin-labeled $HCAII_{67–206}$ with a spin concentration of 0.40 mM in 1:1 buffer glycerol. The data for $T - \tau > 0$ (——) and $T - \tau < 0$ (*light line*) are superimposed on a simulated curve (— — —) that was calculated as described in the text.

Simulated annealing calculations resulted in distances between 7 and 8 Å and a wide range of relative orientations of the inter-spin vector and nitroxyl hyperfine axes. There was no obvious pattern in these orientations. It appears that the dipolar broadening in the spectra of doubly spin-labeled $HCAII_{67–121}$ is not sufficiently well resolved to define these angles. Subtraction of the composite spectrum of $HCAII_{67}$ and $HCAII_{121}$ from the spectrum of $HCAII_{67–121}$ (Fig. 2 *B*) gave the spectrum shown in Fig. 2 *C*. Sharp features in the difference spectrum are attributed to imperfections in the subtractions. The integrated area of the spectrum after subtraction (Fig. 2 *C*) is 62% of the intensity of the original spectrum (Fig. 2 *B*). If all of the sharp signal is attributed to singly labeled protein, this value would indicate a spin-labeling efficiency of 0.62, which is in reasonable agreement with the value of 0.56 obtained by comparison of total spin concentration to total cysteine. The simulated spectrum shown in Fig. 2 *C* was calculated with $r = 8$ Å and line-widths of 20 G. The broad line-width is a surrogate for a distribution in *r* and in relative orientations of the tensors. The feature of the spectrum that is most characteristic of the inter-spin distance is the overall spectral extent.

Distance between labels at positions 59 and 174

The spectrum of doubly labeled $HCAII_{59–174}$ in glassy solution exhibits a broad underlying component, characteristic of a short inter-spin distance (Fig. 3 *A*). Subtraction of

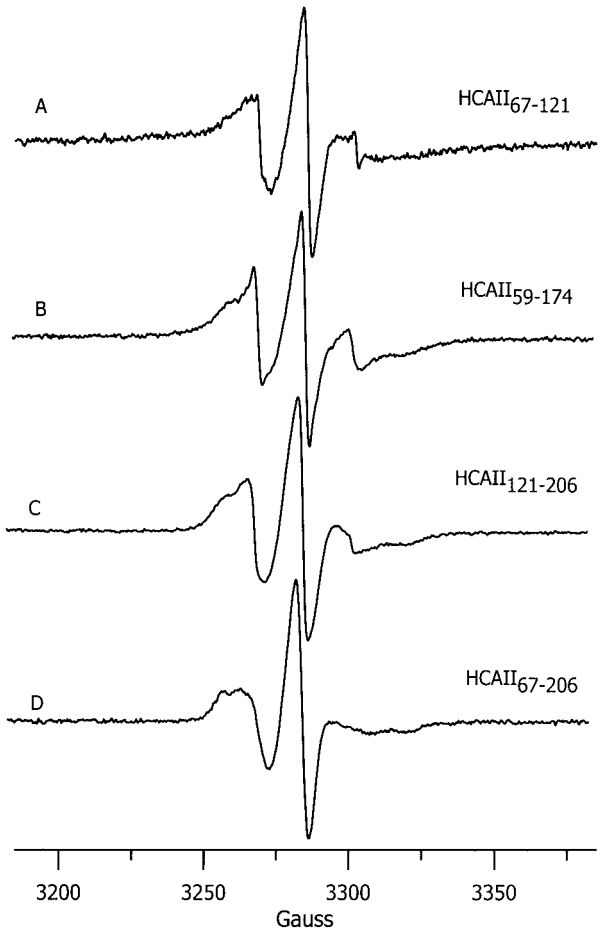

FIGURE 7 Room temperature X-band EPR spectra of doubly spin-labeled HCA II variants in buffer solution. (*A*) $HCAII_{67-121}$ with a spin concentration of 0.58 mM; (*B*) $HCAII_{59-174}$ with a spin concentration of 0.63 mM; (*C*) $HCAII_{121-206}$ with a spin concentration of 0.46 mM; (*D*) $HCAII_{67-206}$ with a spin concentration of 0.80 mM.

a composite spectrum of singly labeled protein from the spectrum of $HCAII_{59-174}$ gave the spectrum shown in Fig. 3 *B*, which has an integrated intensity that is 0.60 times that of the original spectrum. Shin and co-workers (Ottemann et al., 1998) noted that in the Fourier deconvolutions, the limiting (baseline) value of the broadening function in Fourier space reflects the amount of singly labeled protein in the sample. If there were no singly labeled component, the baseline value would be 0. Fourier deconvolution of the spectrum of $HCAII_{59-174}$ (Fig. 3 *A*) gave the broadening function shown in Fig. 3 *C*. The baseline value in Fig. 3 *C* is 0.42 times the initial value, so the fraction of signal due to doubly labeled protein is 0.58, which agrees with the results obtained by subtraction and is consistent with the spin-labeling efficiency calculated from total spin and protein concentrations. Fourier deconvolution of the spectra after subtraction of the sharp component (Fig. 3 *D*) produced a broadening function with baseline approximately zero, as expected. Before, or after, subtraction of the contribution from singly labeled protein the deconvolution method gave inter-spin distances of 8.5–9 Å (Fig. 3, *C* and *D*; Table 1). The relative intensity of the half-field transition gave a distance of 8 Å. Simulation of the line-shape gave an inter-spin distance of 9–10 Å but did not define a unique set of relative orientations. The simulation shown in Fig. 3 *B* was obtained with $r = 9$ Å and Gaussian line-widths of 20 G.

Distance between spin labels at positions 121 and 206

Compared with the spectra for the two HCA II variants shown in Figs. 2 and 3, the glassy spectrum for doubly labeled $HCAII_{121-206}$ shows much less broadening (Fig. 4 *A*). The small broadening, compared with the sum of spectra for the singly labeled analogs, can be seen more clearly in the first integral (absorption) spectra (Fig. 4 *C*). The inter-spin distance in this sample is too long to permit observation of the half-field transition. Fourier deconvolution gave distances in the range of 16–18 Å. The limiting value of the broadening function in Fourier space (Fig. 4 *D*) is 0.15 times the initial value. This corresponds to a spin-labeling efficiency of 0.85, which is in reasonable agreement with the spin-labeling efficiency of 0.88 calculated from total spin concentration and protein concentration. The distances obtained from the line-shape simulations by simulated annealing (Husted method) were very sensitive to model. If it was assumed that there was no singly labeled or long-distance conformation, the inter-spin distance that gave simulated spectra in good agreement with experimental data was 17–19 Å. However, if a singly labeled or longer-distance component was included and the amount of this component was allowed to vary, the distance for the doubly labeled sample was 14–15 Å, and ~45% of the spins were in the singly labeled signal. It appears that the dipolar broadening of the lines in this variant is too small for the simulations to give reliable results if the concentration of the singly labeled component is allowed to vary. The spectrum shown in Fig. 4 *B* was obtained by subtraction of 12% of the composite spectrum of the singly labeled variants. The simulation shown in Fig. 4 *B* was obtained with $r = 16.5$ Å and different line-widths for the two labeling sites, as observed for the corresponding singly labeled proteins. The best-fit distance for this spectrum is quite sensitive to the line-widths assumed for the labels at the two sites.

The DEER data for this sample (Fig. 6) did not show a distinctive modulation pattern, which indicates that there is a relatively wide distribution of inter-spin distances. The simulation shown in Fig. 6 was based on 70% of spins with a distance of 18 Å and 30% with a distance of 24 Å and a 1.5-Å Gaussian distribution width about each of the distances (Table 1). The combined results indicate that there are two distinct sets of conformations of the labels in this sample. The conformations with a distance of ~18 Å can be identified both by Fourier deconvolution and by DEER. The

conformations with the longer distance are defined more clearly by the DEER experiments than in the Fourier deconvolution or line-shape simulations.

Distance between spin labels at positions 67 and 206

CW spectra of doubly labeled $HCAII_{67–206}$ (Fig. 5 *A*) showed little broadening compared with the sum of spectra of the corresponding singly labeled variants. The distance obtained by Fourier deconvolution was dependent on the cutoff value but typically fell between 17 and 20 Å. The limiting value of the broadening function in Fourier space also was dependent on the cutoff value. The limiting value in Fig. 5 *B* is 0.31 times the initial value, indicating that only 69% of the intensity is due to interacting spins. This is significantly lower than the 0.84 spin-labeling efficiency calculated from total spin and protein concentration and suggests that some conformations with relatively long inter-spin distances may be indistinguishable from singly labeled protein in the Fourier analysis. Simulated spectra that agreed well with the experimental data could be obtained for distances between 15 and 24 Å. In this variant, the broadening in the spectrum is so small that it is difficult to distinguish between doubly and singly labeled contributions to the spectrum, although distances obtained by deconvolution were less variable than distances obtained by simulation. The DEER data for this variant (Fig. 6) showed a characteristic modulation pattern that could be simulated with an inter-spin distance of 20 ± 1.8 Å where the stated uncertainty is one standard deviation width of the Gaussian distribution.

Comparison of inter-spin distances with distances between β-carbons

The finite size of the MTSSL spin probe causes the electron-electron inter-spin distances to be significantly different from the distances between the β-carbons of the protein side chain (Table 1). The spin-labeled cysteines that replace Asn-67 and Val-121 in $HCAII_{67–121}$ are located in β-strands 3 and 5, respectively, in a region where the two strands are approximately parallel and both residues point out of the plane that is displayed in Fig. 1. Because the side chains are approximately parallel, it is not surprising that the nitroxyl spin-spin distance in $HCAII_{67–121}$ (7–8 Å) is similar to the distance between the β-carbons in the native amino acids (8.8 Å) that was calculated from the crystal structure (Håkansson et al., 1992). The spin-labeled cysteines that replace Ala-174 and Ile-59 are situated in β-strands 1 and 2, respectively (Fig. 1). Again the labels are in regions where two strands are approximately parallel with the side-chains of Ala-174 and Ile-59 pointing toward the interior of the protein (Fig. 1). Thus, the two labels are probably pointing in a similar direction. In this pair the distance between the native β-carbons is 5.4 Å (Table 1), which is so short that it is not surprising that the two paramagnetic centers are forced to be somewhat further apart (8–10 Å) than the β-carbons. Cys-206 is located toward the end of β-strand 7 in a turn region (Fig. 1), so it is more difficult to describe its orientation relative to Val-121 and Asn-67. The native side chains of Cys-206 and Asn-67 are pointing in similar directions, so the similarity between β-carbon distances (17.9 Å) and spin-spin distances (17–20 Å) seems plausible. The $HCAII_{67–206}$ variant has previously been used for proximity measurements by pyrene labeling (Hammarström et al., 1997). In that study it was found that labels attached to the side chains of these positions were oriented to allow intramolecular excimer formation. Thus, the positions of these side chains of the wild-type residues in the crystal structure should be valid for estimation of the orientation of the attached spin labels at these sites. Of the singly labeled variants examined, the broadest EPR lines were observed for $HCAII_{121}$, which suggests a wider distribution of environments for the label at this location. The DEER data indicate a broad distribution of distances for $HCAII_{121–206}$, which may be due to a range of conformation of the label at the 121 site. Evidence was not obtained for a wide distribution of distances for $HCAII_{67–121}$, which may indicate that the two labeling sites are sufficiently close together that the presence of a label at position 67 restricts the possible conformations at position 121.

In an effort to make these comparisons more rigorously, attempts were made to model the conformation of MTSSL bound to HCA II using the MSI software, Insight II, (Molecular Simulations, San Diego, CA) starting from the x-ray crystal structure (Håkansson et al., 1992). The calculated structures, even after extensive thermal annealing, were strongly dependent upon the initial conformation of the cysteine and attached label and commonly included highly unlikely bond lengths in the vicinity of the label. It appears that the mutations are in sufficiently buried sites of the protein that equilibrium conformations were not achieved in the calculations.

Comparison of methods for distance determination

For each of the variants the inter-spin distance could be obtained by two or three methods, and the results are in reasonable agreement (Table 1). Because spin labeling was not complete, spectra included sharp lines from singly labeled protein. The impact of this spectral component on distance measurements varied with method and inter-spin distance. For $HCAII_{67–121}$ and $HCA_{59–174}$ in which the inter-spin distance is less than 10 Å, the sharp component was readily distinguished from the broadened spectrum of doubly labeled protein. For $HCAII_{121–206}$ and $HCAII_{67–206}$ it was more difficult to distinguish singly labeled protein from conformations with long inter-spin distances. The conclusions discussed below relate to the case of X-band spec-

tra of natural nuclear abundance spin labels in glassy solutions. Some of the limitations observed here might be relaxed by using deuterated labels or by obtaining spectra at additional microwave frequencies (Hustedt et al., 1997).

Measurements of the relative intensity of the half-field transition requires that motion is slow relative to the anisotropy of the half-field transition. The DEER experiment requires a relatively long phase memory time and requires that motion is slow relative to the anisotropy of the small dipolar interactions for long inter-spin distances. These experiments are performed on glassy samples at cryogenic temperatures. To ensure that the state of the sample was the same for all measurements, each sample was quickly frozen in liquid nitrogen and kept frozen during and between measurements. Unlike the half-field and DEER measurements the deconvolution and line-shape simulations can be performed on samples in which motion has been extensively restricted, although not as fully as at lower temperatures, such as by adding high concentrations of glycerol or sucrose and cooling to ~ -30°C. When motion is sufficiently slow, the CW lines for nitroxyl radicals are narrower at -30°C than at temperatures below about -130°C because the rate of rotation of the ring methyl groups at the higher temperatures is fast relative to the inequivalent electron-proton hyperfine interactions (Nakagawa et al., 1992; Barbon et al., 1999). At lower temperatures each proton has a different coupling constant and the resulting inhomogeneous broadening of the line is greater than at higher temperatures. The narrower lines at -30°C than at the -165°C used in the present experiments may permit somewhat longer distances to be determined by line-shape simulation or deconvolution that was possible at the lower temperatures.

Half-field transitions were detected for $HCAII_{67-121}$ and $HCAII_{59-174}$, which have inter-spin distances in the range of 7–8 Å. The integrated intensity of the allowed transitions included spin label on both singly and doubly labeled proteins. An error of up to 20% in the ratio of the integrated intensities caused by inclusion of the contribution from singly labeled protein corresponds to an error of $\sim$0.2 Å at a distance of 7–8 Å. Thus, the distance calculated by this method is relatively insensitive to modest concentrations of singly labeled protein. At the spin concentrations present in the HCA II samples (0.2 to 0.3 mM), the intensity of the half-field transition is low at 7–8 Å and would be difficult to detect at significantly longer distances because the intensity of the half-field transition decreases proportional to r^{-6} (Eaton et al., 1983a). Thus, the utility of this method is greatest at relatively short inter-spin distances, which is the distance range in which it is most important to be able to separate the dipolar interaction and exchange contributions. When there is a distribution of conformations, the dependence of the intensity of the half-field transition on r^{-6} weights the average value strongly toward shorter values. Thus it is not surprising that the values of r for $HCAII_{67-121}$ and $HCAII_{59-174}$ obtained from the half-field transition are on the short end of the ranges obtained by Fourier deconvolution or line-shape simulation (Table 1).

Fourier deconvolution (Rabenstein and Shin, 1995) gave plausible inter-spin distances in the range of $\sim$8–18 Å. The resulting values are dependent on the cutoff frequency in Fourier space, and the sensitivity to cutoff frequency becomes greater at longer inter-spin distances. When the dipolar broadening is large, the calculated distance is not strongly dependent upon which singly labeled variant, or combination of variants, is used for the deconvolution. However, as the broadening becomes smaller, it is increasingly important to have accurate information on the line-shape in the absence of spin-spin interaction. In the shorter distance end of this range, deconvolution appears to distinguish cleanly between the most strongly broadened component of the spectrum and other contributions with minimal broadening due to singly labeled protein. As the inter-spin distance becomes longer it becomes more difficult to distinguish between contributions from singly labeled protein and conformations with longer inter-spin distance. Constraints on the two contributions can be obtained by comparison of the limiting value in the Fourier broadening function with the contribution expected based on independent measures of spin-labeling efficiency. The Fourier deconvolution method assumes that there is a random distribution of relative orientations of the nitroxyl hyperfine axes relative to the inter-spin vector. In the crystal structures of several spin-labeled variants of T4 lysozyme, the electron density for the nitroxyl ring was poorly defined, consistent with a distribution of conformations (Langen et al., 2000).

For the samples with distances of $\sim$7–9 Å, line-shape simulation with simulated annealing (Hustedt et al., 1997) gave families of solutions with a relatively narrow range of values of inter-spin distance and a wide range of angular parameters. The broad contribution from doubly labeled protein could be distinguished from singly labeled protein, and the resulting fit parameters for the interacting component were in reasonable agreement with the signal that was obtained after subtraction of the sharp component (Figs. 2 *C* and 3 *B*). However, at the longer distances of 16–20 Å for $HCAII_{121-206}$ or $HCAII_{67-206}$, the dipolar broadening was too small to generate clearly distinguishable features, and apparently acceptable simulated spectra could be obtained with a wide range of inter-spin distances. These observations suggest that for samples with natural isotope-abundance spin labels and containing some singly labeled protein, the present line-shape simulations of spectra in glassy solutions at low temperature are not reliable at X-band for distances longer than $\sim$15 Å. The simulation programs used in this study assume that there is a unique set of angular parameters (five Euler angles) that define the relative orientations of the nitroxyl hyperfine axes and the inter-spin vector (Hustedt et al., 1997). This assumption is the opposite of the random distribution of relative orientation assumed for the Fourier deconvolution procedure (Rabenstein

and Shin, 1995). The agreement in the inter-spin distances obtained by the two approaches suggests that when the dipolar splittings are not well resolved, as in the spectra for the HCA II samples, these assumptions are not key to obtaining useful distance information.

As currently implemented on our spectrometer the four-pulse DEER method (Pannier et al., 2000) is limited to distances longer than ~18 Å. For measurement of the $HCAII_{121–206}$ and $HCAII_{67–206}$ distances the DEER experiments were more informative than either deconvolution or line-shape simulation. The DEER method has the advantage that the characteristic oscillations arise only from doubly labeled protein, and the presence in the sample of singly labeled protein does not complicate the data analysis. In addition, the rate at which the oscillation damps provides a more direct indication of the widths of distance distributions than is currently available from CW line-shapes by either simulation or deconvolution.

CONCLUSIONS

The inter-spin distances obtained by several EPR methods are in reasonable agreement. The useful distance ranges for the techniques examined at X-band in glassy solvent with natural isotope-abundance labels for samples that contain some singly labeled protein are approximately as follows: half-field transition (5–10 Å), line-shape simulation (up to 15 Å), Fourier deconvolution (8–20 Å), and four-pulse DEER (>18 Å). By using multiple techniques a more complete picture is obtained than can be found by a single technique.

We thank Dr. Angela Zhou for help with attempts to use the molecular modeling program Insight, Dr. Eric Hustedt for help with the line-shape simulation programs, Prof. H. Spiess and Dr. G. Jeschke for advice on the DEER method and for a sample of their biradical 3, and Dr. Mikael Lindgren for valuable discussions.

This work was supported by grants from the National Institutes of Health (GM21156 and GM54331 to S.S.E. and G.R.E.), The Wenner-Gren Foundation and The Blancheflor Boncompagni-Ludovisi, née Bildt (M.P. and P.H.), The Swedish Natural Science Research Council (U.C.), Helge Ax:son Johnson's Foundation (P.H.), and Lars Hierta's Memorial Foundation (P.H.).

REFERENCES

Alexander, R. S., S. K. Nair, and D. W. Christianson. 1991. Engineering the hydrophobic pocket of carbonic anhydrase II. *Biochemistry.* 30: 11064–11072.

Barbon, A., M. Brustolon, A. L. Maniero, M. Romanelli, and L.-C. Brunel. 1999. Dynamics and spin relaxation of Tempone in a host crystal: an ENDOR, high-field EPR, and electron spin echo study. *Phys. Chem. Chem. Phys.* 1:4015–4023.

Borbat, P. P., and J. H. Freed. 1999. Multi-quantum ESR and distance measurements. *Chem. Phys. Lett.* 313:145–154.

Eaton, S. S., K. M. More, B. M. Sawant, and G. R. Eaton. 1983a. Use of the EPR half-field transition to determine the interspin distance and the orientation of the interspin vector in systems with two unpaired electrons. *J. Am. Chem. Soc.* 105:6560–6567.

Eaton, S. S., K. M. More, B. M. Sawant, P. M. Boymel, and G. R. Eaton. 1983b. Metal-nitroxyl interactions. 29. EPR studies of spin-labeled copper complexes in frozen solution. *J. Magn. Reson.* 52:435–449.

Eriksson, A. E., T. A. Jones, and A. Liljas. 1988. Refined structure of human carbonic anhydrase II at 2.0 Å resolution. *Proteins Struct. Funct. Genet.* 4:274–282.

Fierke, C. A., T. L. Calderone, and J. F. Krebs. 1991. Functional consequences of engineering the hydrophobic pocket of carbonic anhydrase II. *Biochemistry.* 30:11054–11063.

Freskgård, P.-O., U. Carlsson, L.-G. Mårtensson, and B.-H. Jonsson. 1991. Folding around the C-terminus of human carbonic anhydrase II. *FEBS Lett.* 289:117–122.

Freskgård, P. O., L.-G. Mårtensson, P. Jonasson, B. H. Jonsson, and U. Carlsson. 1994. Assignment of the contribution of the tryptophan residues to the circular dichroism spectrum of human carbonic anhydrase II. *Biochemistry.* 33:14281–14288.

Grassetti, D. R., and J. F. Murray, Jr. 1967. Determination of sulfhydryl groups with 2,2′ and 4,4′-dithiopyridine. *Arch. Biochem. Biophys.* 119: 41–49.

Håkansson, K., U. Carlsson, M. Svensson, and A. Liljas. 1992. Structure of native and apo carbonic anhydrase II and structure of some of its anion-ligand complexes. *J. Mol. Biol.* 277:1192–1204.

Hammarström, P., B. Kalman, B.-H. Jonsson, and U. Carlsson. 1997. Pyrene excimer fluorescence as a proximity probe for investigation of residual structure in the unfolded state of human carbonic anhydrase II. *FEBS Lett.* 420:63–68.

Henderson, L. E., D. Henriksson, and P. O. Nyman. 1976. Primary structure of human carbonic anhydrase C. *J. Biol. Chem.* 251:5457–5463.

Hubbell, W. L., and C. Altenbach. 1994. Investigation of structure and dynamics of membrane proteins using site-directed spin labeling. *Curr. Opin. Struct. Biol.* 4:566–573.

Hubbell, W. L., A. Fross, R. Langren, and M. A. Lietzow. 1998. Recent advances in site-directed spin labeling of proteins. *Curr. Opin. Struct. Biol.* 8:649–656.

Hunt, J. A., M. Ahmed, and C. A. Fierke. 1999. Metal binding specificity in carbonic anhydrase is influenced by conserved hydrophobic core residues. *Biochemistry.* 38:9054–9062.

Hustedt, E. J., C. E. Cobb, A. H. Beth, and J. M. Beechem. 1993. Measurement of rotational dynamics by the simultaneous nonlinear analysis of optical and EPR data. *Biophys. J.* 64:614–621.

Hustedt, E. J., A. I. Smirnov, C. F. Laub, C. E. Cobb, and A. H. Beth. 1997. Molecular distances from dipolar coupled spin-labels: the global analysis of multifrequency continuous wave electron paramagnetic resonance data. *Biophys. J.* 74:1861–1877.

Khalifah, R. G., D. J. Strader, S. H. Bryant, and S. M. Gibson. 1977. Carbon-13 nuclear magnetic resonance probe of active-site ionizations in human carbonic anhydrase B. *Biochemistry.* 16:2241–2247.

Kokorin, A. I., K. I. Zamarayev, G. L. Grigoryan, V. P. Ivanov, and E. G. Rozantsev. 1972. Measurement of the distances between the paramagnetic centers in solid solutions of nitroxide radicals, biradicals, and spin-labeled proteins. *Biofizika.* 17:34–41.

Kunkel, T. A., J. D. Roberts, and R. A. Zakour. 1987. Rapid and efficient site-specific mutagenesis without phenotypic selection. *Methods Enzymol.* 154:367–382.

Langen, R., K. J. Oh, D. Cascico, and W. L. Hubbell. 2000. Crystal structures of spin labeled T4 lysozyme mutants: implications for the interpretation of EPR spectra in terms of structure. *Biochemistry.* 39: 8396–8405.

Larsen, R. G., and D. J. Singel. 1993. Double electron-electron resonance spin-echo modulation: spectroscopic measurement of electron spin pair separations in orientationally disordered solids. *J. Chem. Phys.* 98: 5134–5146.

Lindgren, M., M. Svensson, P.-O. Freskgård, U. Carlsson, B.-H. Jonsson, L.-G. Mårtensson, and P. Jonasson. 1993. Probing local mobility in carbonic anhydrase: EPR of spin-labeled SH groups introduced by site-directed mutagenesis. *J. Chem. Soc. Perkin Trans.* 2:2003–2007.

Lindskog, S. 1997. Structure and mechanism of carbonic anhydrase. *Pharmacol. Ther.* 74:1–20.

Mårtensson, L.-G., B.-H. Jonsson, P.-O. Freskgård, A. Kihlgren, M. Svensson, and U. Carlsson. 1993. Characterization of folding intermediates of human carbonic anhydrase II: probing substructure by chemical labeling of sulfhydryl groups introduced by site-directed mutagenesis. *Biochemistry.* 32:224–231.

Martin, R. E., M. Pannier, F. Diederich, V. Gramlich, M. Hubrich, and H. W. Spiess. 1998. Determination of the end-to-end distances in a series of TEMPO diradicals of up to 2.8 nm length with a new four-pulse double electron electron resonance experiment. *Angew. Chem.* 37: 2834–2837.

Mchaourab, H. S., M. A. Lietzow, K. Hideg, and W. L. Hubbell. 1996. Motion of spin-labeled side chains in T4 lysozyme: correlation with protein structure and dynamics. *Biochemistry.* 35:7692–7704.

Milov, A. D., A. G. Maryanov, and Yu. D. Tsvetkov. 1998. Pulsed electron double resonance (PELDOR) and its application in free radicals research. *Appl. Magn. Reson.* 15:107–143.

Milov, A. D., K. M. Salikhov, and M. D. Shirov. 1981. Application of the double resonance method to electron spin echo in a study of the spatial distribution of paramagnetic centers in solids. *Sov. Phys. Solid State.* 23:565–569.

Nair, S. K., T. L. Calderone, D. W. Christianson, and C. A. Fierke. 1991. Altering the mouth of a hydrophobic pocket: structure and kinetics of human carbonic anhydrase II mutants at residue Val-121. *J. Biol. Chem.* 266:17320–17325.

Nakagawa, K., M. B. Candelaria, W. W. C. Chik, S. S. Eaton, and G. R. Eaton. 1992. Electron spin relaxation times of chromium(V). *J. Magn. Reson.* 98:81–91.

Nyman, P. O., and S. Lindskog. 1964. Amino acid composition of various forms of bovine and human erythrocyte carbonic anhydrase. *Biochim. Biophys. Acta.* 85:141–151.

Ottemann, K. M., T. E. Thorgeirsson, A. F. Kolodziej, Y.-K. Shin, and D. E. Koshland, Jr. 1998. Direct measurement of small ligand-induced conformational changes in the aspartate chemoreceptor using EPR. *Biochemistry.* 37:7062–7069.

Pannier, M., S. Veit, A. Godt, G. Jeschke, and H. W. Spiess. 2000. Dead-time free measurement of dipole-dipole interactions between electron spins. *J. Magn. Reson.* 142:331–340.

Persson, M. P., P. Hammarström, M. Lindgren, B.-H. Jonsson, M. Svensson, and U. Carlsson. 1999. EPR mapping of interactions between spin-labeled variants of human carbonic anhydrase II and GroEL: evidence for increased flexibility of the hydrophobic core by the interaction. *Biochemistry.* 38:432–441.

Quine, R. W., G. R. Eaton, and S. S. Eaton. 1987. Pulsed EPR spectrometer. *Rev. Sci. Instrum.* 58:1709–1724.

Rabenstein, M. D., and Y.-K. Shin. 1995. Determination of the distance between two spin labels attached to a macromolecule. *Proc. Natl. Acad. Sci. U.S.A.* 92:8239–8243.

Raitsimring, A., J. Peisach, H. C. Lee, and X. Chen. 1992. Measurement of distance distributions between spin labels in spin-labeled hemoglobin using an electron spin echo method. *J. Phys. Chem.* 96:3526–3531.

Rickli, E. E., S. A. S. Ghanzafar, B. H. Gibbon, and J. T. Edsall. 1964. Carbonic anhydrases from human erythrocytes *J. Biol. Chem.* 239: 1065–1078.

Rinard, G. A., R. W. Quine, J. R. Harbridge, R. Song, G. R. Eaton, and S. S. Eaton. 1999. Frequency dependence of EPR signal-to-noise. *J. Magn. Reson*. 140:218–227.

Sanger, F., S. Nicklen, and A. R. Coulson. 1977. DNA sequencing with chain-terminating inhibitors. *Proc. Natl. Acad. Sci. U.S.A.* 74: 5463–5467.

Saxena, S., and J. H. Freed. 1997. Theory of double quantum two-dimensional electron spin resonance with application to distance measurements. *J. Chem. Phys.* 107:1317–1340.

Sun, J., J. Voss, W. L. Hubbell, and H. R. Kaback. 1999. Proximity between periplasmic loops in the lactose permease of *Escherichia coli* as determined by site-directed spin labeling. *Biochemistry.* 38:3100–3105.

Svensson, M., P. Jonasson, P.-O. Freskgård, B.-H. Jonsson, M. Lindgren, L.-G. Mårtensson, M. Gentile, K. Boren, and U. Carlsson. 1995. Mapping the folding intermediate of human carbonic anhydrase II: probing substructure by chemical reactivity and spin and fluorescence labeling of engineered cysteine residues. *Biochemistry.* 34:8606–8620.

Toy, A. D., S. H. H. Chaston, J. R. Pilbrow, and T. D. Smith. 1971. An electron spin resonance study of the copper(II) chelates of certain monothio-β-diketonates and diethyldithiocarbamate. *Inorg. Chem.* 10: 2219–2225.